This is to certify that the

dissertation entitled

Numerical Computations in Electromagnetics: A Direct Problem in Magnetic Recording and an Inverse Problem in Medical Imaging

presented by

John L. Fleming

has been accepted towards fulfillment
of the requirements for

Ph.D. degree in Mathematics

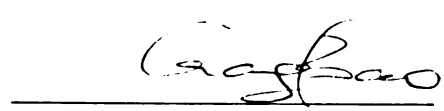

Major professor

Date December 5, 2001

Numerical Computations in Electromagnetics: A Direct Problem in Magnetic Recording and An Inverse Problem in Medical Imaging

By

John L. Fleming

A DISSERTATION

Submitted to
Michigan State University
in partial fulfillment of the requirements
for the degree of

DOCTOR OF PHILOSOPHY

Department of Mathematics

2001

ABSTRACT

Numerical Computations in Electromagnetics: A Direct Problem in Magnetic Recording and An Inverse Problem in Medical Imaging

By

John L. Fleming

The thesis will discuss two problems from the world of electromagnetics. The first problem is a direct problem with applications in magnetic recording. It focuses on a computation of magnetic field in an infinite cavity. The basic solution method is a Fourier approach. Numerical analysis of the method involves the study of an infinite matrix and issues surrounding the truncation of the matrix. The second problem is an inverse problem in electromagnetics. The inverse method computes the position and orientation of a dipole current source in a conducting medium using boundary measurements of the electromagnetic fields. The method is an asymptotic approach based on a low frequency assumption. The inverse method has applications in medical imaging.

To all of my family and friends.

ACKNOWLEDGMENTS

First and foremost I would like to thank my advisor Gang Bao for supporting me, introducing me to many interesting subjects and providing many opportunities. Also, I thank Tri Van and Leo Kempel for their time and assistance with many questions. In addition, I thank the additional members of my commitee Zhengfou Zhou, Baisheng Yan and Chichia Chiu. Finally, I thank my parents, William and Elizabeth Fleming, for supporting me in all my endeavors

TABLE OF CONTENTS

Introduction

The field of electromagnetics was one of the most important scientific fields of the 20th century. It changed the landscape of modern society. The understanding of electromagnetic fields has permeated almost every aspect of culture in the modern world. Scientists facilitated the development of the modern electromagnetic world through physical reasoning and experimentation. Mathematicians have also been very important to the development of the field as well. As a mathematician, one can help with the physical reasoning and development of models, but the unique contribution which can be made is to offer an understanding of physical models from a mathematical point of view as well as to provide insight into mathematical issues surrounding the models such as convergence, stability, existence and uniqueness.

In this thesis, two particular models of electromagnetic phenomenon will be studied. One is a direct problem, which has applications in the world of computers. The problem studies a model used to simulate certain interactions occurring in magnetic recording devices. Here the problem will have certain parameters which will be used to compute the magnetic field produced. The second problem is an inverse problem with applications in the world of biomedical imaging. Here values of the electromagnetic fields will be provided and the solution will be the computation of certain parameters which are of interest.

In the direct problem, the thesis will recount a Fourier series approach to a problem in magnetic recording. The method was provided by engineers in the paper [24]. As

with many engineering approaches, much is left to be desired from a mathematical point of view. The method has no rigorous derivation or convergence theory, both of which are always very important when the method will be used and trusted by those in industry. In particular, it will be shown that the method involves a somewhat unusual infinite dimensional matrix. In actual computations one must truncate the infinite matrix. Unfortunately, this raises many questions as to the validity and accuracy of the truncation. The contribution here will be to reveal insight into the mysterious infinite matrix by using a more familiar variational approach and then finding a parallel between the two. Finding this connection allows for a thorough analysis that would otherwise not be forthcoming from direct analysis of the Fourier method. Also, we will see that the variational form of the problem allows for a more general finite element solution approach. The finite element technique would allow for computations that could not be done with the Fourier method. Hence the thesis clearly provides new insight mathematically into the Fourier computational technique. Also, it provides a more flexible approach in the form of a finite element formulation.

In the inverse problem, the thesis will present a novel frequency based approach to a dipole source problem [2]. The goal is to reconstruct the location and orientation of a dipole current source in a conducting volume using only measurements of the tangential components of the magnetic and electric fields on the boundary of the volume. It is known that neurological disease epilepsy is often caused by a small current discharge in the brain. Such small current discharges can be reasonably modeled as a dipole current source. While treatable with medication, the disease is only permanently curable by surgical removal. Hence, precise knowledge of the dipole location is of vital importance. Medical professionals can measure electric and magnetic fields from the human brain using magnetoencephalography and electroencephalography. Medical imaging uses these measurements to diagnose various conditions of the brain. The goal here is to use these type of measurements to locate a dipole source

in the brain which is an inhomogeneous conducting material. The only bit of *a priori* knowledge about the dipole is the fact that the frequency will be very low. Since the frequency is known to be very low, this motivates an asymptotic approach. That is to say we want an approach for which the accuracy improves as the frequency approaches zero. The contribution in the thesis will be numerical experiments of several varieties. Also, it will be demonstrated how the method can be used to compute the parameters of multiple dipoles in a conducting volume.

Most techniques to solve this type of inverse point source problem are iterative techniques [21][12]. The problem with these methods is that the iterations can be time consuming and computationally unattractive. Also, they suffer from a lack of stability in the presence of noisy data. Even noniterative techniques in this area lack rigorous mathematical analysis. [14] The asymptotic method presented here is noniterative and also has a strong mathematical foundation.

The two problems studied here are just a small glimpse into two areas of the large field of electromagnetics. However, as the understanding of electromagnetic problems becomes more prominent in the world, every small contribution will be important for completing the understanding of all aspects of the field. The mathematician's input should be to use their unique insight to prove that computational models and methods are valid and dependable.

CHAPTER 1

Fundamentals

1.1 Maxwell's equations

The foundation of the modern theory of electromagnetics is the Maxwell's equations. The following equations and parameters are the basis for the wave theory of electromagnetics.

$$\nabla \times \vec{E} = -\epsilon \frac{\partial \vec{H}}{\partial t} + \vec{M} \tag{1.1}$$

$$\nabla \times \vec{H} = \mu \frac{\partial \vec{E}}{\partial t} + \vec{J} \tag{1.2}$$

$$\nabla \cdot \vec{E} = \rho_e \tag{1.3}$$

$$\nabla \cdot \vec{H} = -\nabla \cdot \vec{M} = \rho_m \tag{1.4}$$

$\vec{E}$ - Electric Field

$\vec{H}$ - Magnetic Field

$\vec{J}$ - Electric Current

$\vec{M}$ - Magnetization

ρ_e - Electric Charge

ρ_m - Magnetic Charge

ϵ - Electric Permitivity

μ - Magnetic Permeability

The solution of the direct problem regarding Maxwell's equations is to find $\vec{E}$ and $\vec{H}$ given $\vec{M}$, $\vec{J}$, ρ, ρ_m, ϵ and μ. The computational approach is solving the differential equations in a given region with knowledge of appropriate boundary conditions for $\vec{E}$ and $\vec{H}$. The inverse problem would be to compute something about the $\vec{J}$,$\vec{M}$,ρ,ρ_m, ϵ or μ given particular values of $\vec{E}$ or H. In this thesis, the interest will be focused on computing information about a certain type of current $\vec{J}$ within a volume given measurements of $n \times \vec{E}$ and $n \times \vec{H}$ on the boundary of the volume.

Often, the time harmonic formulation is used. The time harmonic formulation means that the fields are assumed to have an exponential time dependance. That is $\vec{E}(x,y,z,t) = \vec{E}(x,y,z)e^{-i\omega t}$ and $\vec{H}(x,y,z,t) = \vec{H}(x,y,z)e^{-i\omega t}$. Thus the time derivatives will produce a factor of $-i\omega$. Therefore. the time-harmonic form of the Maxwell's equations are as follows.

$$\nabla \times \vec{E} = -i\omega\epsilon \vec{H} + \vec{M} \tag{1.5}$$

$$\nabla \times \vec{H} = -i\omega\mu \vec{E} + \vec{J} \tag{1.6}$$

$$\nabla \cdot \vec{E} = \rho_e \tag{1.7}$$

$$\nabla \cdot \vec{H} = -\nabla \cdot \vec{M} = \rho_m \tag{1.8}$$

In chapter 3 these time harmonic equations will be used in the analysis of an inverse point source problem. In particular, the case where ω is very low will be considered.

1.2 Potential formulation

If the frequency ω is zero, this is know as the quasi-static form of Maxwell's equations. The equation (1.1) becomes

$$\nabla \times \vec{E} = 0 \tag{1.9}$$

Hence, we know that $\vec{E} = \text{grad}\phi$ for some scalar function ϕ. Using this along with (1.3) we have

$$\triangle \phi = \rho_e \tag{1.10}$$

Also, If the region of interest is free of current ($\vec{J} = 0$) then (1.2) is

$$\nabla \times \vec{H} = 0. \tag{1.11}$$

Therefore, a magnetic scalar potential equation ϕ_m can be constructed in a similar manner.

In chapter 2, the scalar magnetic potential equation will be used to compute magnetic fields. A solution method will be studied for the Laplace equation with appropriate boundary conditions. Of particular interest will be what happens to the solution at the transition from an infinite half space to a space with support on a finite interval.

CHAPTER 2

Fourier Series Method

2.1 Introduction

Magnetic recording is one of the fundamental technologies behind the modern computer. Massive amounts of information are stored on magnetic media called disk drives. In this chapter, the basics principles of magnetic recording will be introduced. In particular, the process of the head media interaction will be modeled mathematically using the Fourier series method [24] [15]. The thrust of the chapter is to analyze this method mathematically.

2.2 Magnetic Recording

Inside every modern computer is a magnetic storage device known as the computer's hard drive. Figure 2.2 shows a picture of a typical hard drive and also a hard drive with the inside exposed. Within the casing of the drive are a series of disks. The disks are made up of magnetic media on which binary information is stored. The magnetic media is divided into sectors. Each sector has its own magnetization. Suspended over the magnetic media is a slider mechanism which houses the recording head. The recording head is a device which reads and writes the information on the disk. The

read device employs a thin film know as a magnetoresistive (MR) head. The MR head is sandwiched between two magnetic shields to focus it on the area directly below. As the MR head moves over the magnetic media, it can detect the presence of magnetic fields produced by the magnetization of the media. If the magnetization on the media changes across a transition from one sector to another, this represents the binary digit 1. If there is no change across the transition, this represents the binary digit 0 [30]. The process is illustrated in figure 2.4.

In the magnetic recording industry, manufacturers are always interested in testing new ideas and new technology. However, to save on production costs and development time, it is important to model the systems whenever possible. In this chapter the head media interaction is modeled and solved using a Fourier approach. The contribution of the thesis is an analysis of the problem mathematically. We shall see that the computation method involves truncating an infinite matrix. There is no established result regarding this type of estimation. It is both important from a computational point of view to understand the consequences of truncating the matrix, but it is also interesting from a purely mathematical perspective to understand just what is lost by approximating the infinite matrix with a finite truncation.

2.3 The Model of Head Media Interaction

When constructing the mathematical model, there will be a number of simplifying assumptions. The assumptions allow the problem to be modeled more easily, without making the model too unrealistic.

Assumptions:

1. Field is Static (Time derivatives are zero). Even though the interaction is a dynamic process, it is the assumption that the drive moves slow enough to be approximately static.

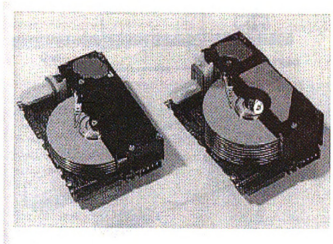

Figure 2.1. A picture of a typical computer hard drive with the inside exposed [30].

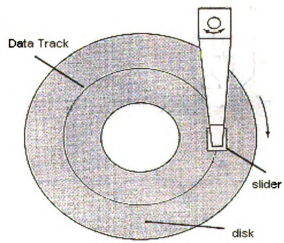

Figure 2.2. Diagram of the disk media and the slider mechanism [30].

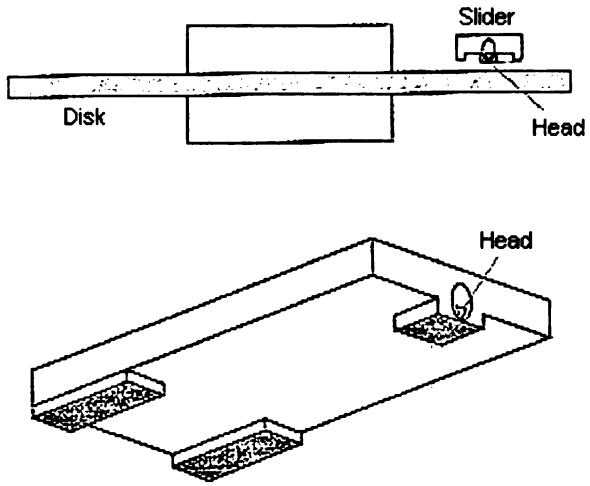

Figure 2.3. A closer view of the slider and the head read-write head [30].

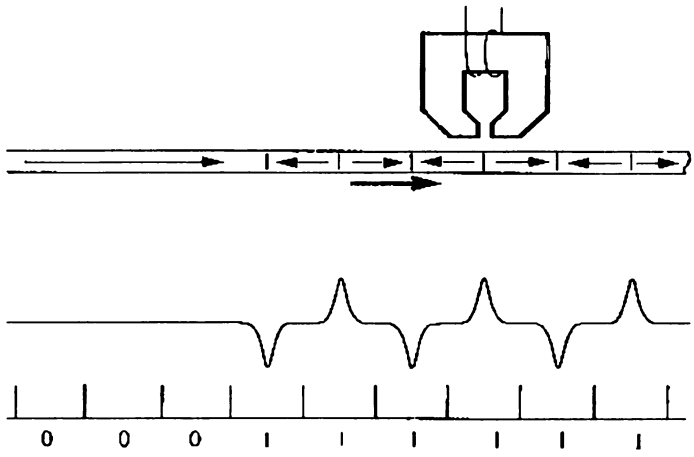

Figure 2.4. Head media interaction [30].

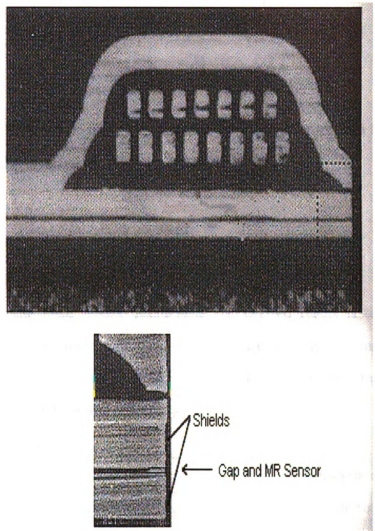

Figure 2.5. A very close up view of an actual read-write head [30].

2. There is no electric charge or current ($\rho_e = 0$) and $\left(\vec{J} = 0\right)$. Thus, from (1.2) for the magnetic field, we have $\nabla \times H = 0$.

As was seen in chapter 1, this implies $H = \nabla\phi_m$. where the scalar function ϕ_m is known as the magnetic scalar potential. Recall also that given (1.4) we see ϕ_m satisfies Poisson's equation

$$\triangle\phi_m = \rho_m. \tag{2.1}$$

Note that given a magnetic charge ρ_m in free space, the solution can be found using an appropriate Green's function by the following [27]:

$$\phi_m(\vec{x}) = \iint_{S_0} \rho_m(x_0)G(x, x_0)dS_0 \tag{2.2}$$

When modeling the head media interaction, the desired result is to compute the magnetic fields in the shield gap (region I in figure 2.6) due to magnetic charge outside (below) the gap (region II in fig 2.6). For the model, we will make some more assumptions which simplify the solution process.

More assumptions:

1. The problem is invariant in the z-direction. (2-D). The analysis of the problem will be given for the two dimensional case. However, we will be able to solve the three dimensional problem with the Fourier method as well.

2. The shields are infinite in both the x and y directions. In reality the shields are much larger than the gap spacing, so this is a reasonable assumption to simplify the mathematics. In figure 2.2 it can be seen how much larger the shields are compared to the gap spacing. Also, the shields are assumed to have an infinite permeability. That is to say the magnetic field, H, is zero in the shields.

3. Assume there is no MR-film. It is assumed that the gap spacing is empty. This assumption allows the use of the Fourier method. However, the analysis will show that a convienient finite element method can be devised which would allow for modelling the problem with inhomogeneous materials in the gap.

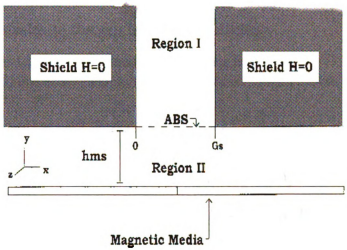

Figure 2.6. Illustration of the problem.

Note, that away from the charge distribution, the potential will satisfy Laplace's equation ($\triangle\phi_m = 0$). Since there is no charge inside the gap, this is the situation we have. The rectangular geometry makes the use of Fourier theory a natural approach to find the solution.

2.4 Fourier Component Formulation

The Fourier based solution method was offered in [24]. The method presented, or very similar methods, have been used within several models [15][24]. These engineering papers offer a pragmatic method for finding the solution with Fourier theory, but offer no justification of some important details of the method. The most interesting aspect of the method is what happens at the transition from the infinite lower half space below the shields to the gap between the shields.

In region I the solution will have the following form

$$\phi_I = \sum_{n=1}^{\infty} A_n \sin\left(\frac{n\pi x}{G_s}\right) \mathrm{e}^{-\left(\frac{n\pi}{G_s}\right)y} \tag{2.3}$$

Since the support of the potential in the x-direction, is only in the interval from 0 to G_s, a Fourier series can be used. On the other hand in region II the solution has the form

$$\phi_{II} = \int_{-\infty}^{+\infty} \left(B(k_x)e^{-\kappa y} + C(k_x)\mathrm{e}^{\kappa y}\right) \mathrm{e}^{2\pi i k_x x} \mathrm{d}k_x \tag{2.4}$$

(Where $\kappa = |2\pi k_x|$) Since the support in the x direction is now infinite, a Fourier transform must be used instead of a Fourier series to express the solution. The interesting part of the problem comes from coupling the two forms of the solution together at the gap interface.

We can compute the potential without the presence of shields (this will be denoted by ϕ_0) using (2.2). Note that in terms of the Fourier components

$$\phi_0 = \int_{-\infty}^{+\infty} B(k_x)e^{-\kappa y}\mathrm{d}k_x. \tag{2.5}$$

This is true because this portion of the potential must decay as y increases to be

physically reasonable.

Also, note that the potential reflected from the shield in region II (ϕ_r) is

$$\phi_r = \int_{-\infty}^{+\infty} C(k_x) e^{\kappa y} \mathrm{d}k_x \tag{2.6}$$

because this portion of the solution must decay as y decreases in order to be physically reasonable. The total solution in region II is simply the superposition of the potentials ϕ_0 and ϕ_r.

Recall that the main problem is to compute the potential in region I given a charge distribution ρ in region II. In terms of the Fourier approach, we must compute the Fourier coefficients A_n in 2.3.

2.5 Solution Method

A method to compute the Fourier coefficients was presented in the paper [24].

Examine what happens at the interface between the gap in region I and the lower half-plane of region II. The two forms of the solution will satisfy some standard continuity conditions.

First, the potential is continuous at the gap interface. This fact gives the following equation

$$\phi_I|_{y=0} = \phi_{II}|_{y=0}\,. \tag{2.7}$$

Second, the normal derivative $\left(\frac{\partial}{\partial y}\right)$ is continuous across the gap interface. Hence, we have the equation

$$\left.\frac{\partial \phi_I}{\partial y}\right|_{y=0} = \left.\frac{\partial \phi_{II}}{\partial y}\right|_{y=0} \tag{2.8}$$

Using the forms of the solution in the respective regions (2.3) and (2.4) and the previous two equations from the continuity conditions an expression that determines the A_n can be found.

The first continuity equation gives the following:

$$\sum_{n=1}^{\infty} A_n \sin\left(\frac{n\pi x}{G_s}\right) = \int_{-\infty}^{+\infty} (B + C)\, \mathrm{e}^{2\pi i k_x x} \mathrm{d}k_x \tag{2.9}$$

or

$$\sum_{n=1}^{\infty} A_n \sin\left(\frac{n\pi x}{G_s}\right) = \mathcal{F}_x^{-1}(B + C) \tag{2.10}$$

Taking the Fourier Transform in the x-direction of both sides gives

$$\sum_{n=1}^{\infty} A_n \mathcal{F}_x\left(\sin\left(\frac{n\pi x}{G_s}\right)\right) = (B + C) \tag{2.11}$$

or

$$\mathcal{F}_x(\phi_I) = B + C \tag{2.12}$$

Note that both the A_n's and C are unknown. Hence, it is necessary to eliminate C which allows for the determination of the A_n's in terms of the known quantity B. This is accomplished from the second continuity condition.

The second continuity condition gives the following:

$$\sum_{n=1}^{\infty} \left(\frac{-n\pi}{G_s}\right) A_n \sin\left(\frac{n\pi x}{G_s}\right) = \int_{-\infty}^{+\infty} (-\kappa B + \kappa C)\, \mathrm{e}^{2\pi i k_x x} \mathrm{d}k_x \tag{2.13}$$

or

$$\sum_{n=1}^{\infty}\left(\frac{-n\pi}{G_s}\right)A_n\sin\left(\frac{n\pi x}{G_s}\right)=\mathcal{F}_x^{-1}(-\kappa B+\kappa C) \tag{2.14}$$

Multiplying both sides of the previous equation by $\sin(\frac{m\pi x}{G_s})$ and integrating from 0 to G_s gives the following:

$$-\left(\frac{2}{G_s}\right)\left(\frac{m\pi}{G_s}\right)A_m=\int_0^{G_s}\mathcal{F}_x^{-1}\left(-\kappa B+\kappa C\right)\sin\left(\frac{m\pi x}{G_s}\right)\mathrm{d}x \tag{2.15}$$

Solve for C in (2.12) and substitute into (2.15) to arrive at the following:

$$\frac{-2m\pi}{G_s^2}A_m=\int_0^{G_s}\mathcal{F}_x^{-1}\big[-2\kappa B+\sum_{n=1}^{\infty}A_n\mathcal{F}_x\left(\sin\left(\frac{n\pi x}{G_s}\right)\right)\big]\sin\left(\frac{m\pi x}{G_s}\right)\mathrm{d}x \tag{2.16}$$

By Parseval's formula, we have

$$\frac{-2m\pi}{G_s^2}A_m=-B_m+\sum_{n=1}^{\infty}K_{mn}\,A_n \tag{2.17}$$

where

$$B_m=\int_{-\infty}^{+\infty}2B\,\mathcal{F}_x^{-1}\left(\sin\left(\frac{m\pi x}{G_s}\right)\right)\mathrm{d}k_x \tag{2.18}$$

and

$$K_{nm}=\int_{-\infty}^{+\infty}\kappa\mathcal{F}_x\left(\sin\left(\frac{n\pi x}{G_s}\right)\right)\mathcal{F}_x^{-1}\left(\sin\left(\frac{m\pi x}{G_s}\right)\right)\mathrm{d}k_x \tag{2.19}$$

Thus, we have a formulation of the Fourier coefficients in terms of the Fourier transform B. However, we see that the Fourier coefficients of ϕ_I satisfy an infinite

system of linear equation given by (2.17).

$$\widetilde{K}\left\{\overline{A}\right\} = \left\{\overline{B}\right\} \tag{2.20}$$

Where $\widetilde{K}_{nm} = K_{nm} + \frac{-2m\pi}{G_s^2}\delta_{nm}$. For purposes of computation such an infinite matrix does no good. It is not reasonable to deal with such a mathematical structure. An obvious response to deal with the situation is to solve a truncated version of the infinite matrix.

$$\widetilde{K_N}\left\{\overline{A_N}\right\} = \left\{\overline{B_N}\right\} \tag{2.21}$$

Even though this seems to be the logical approach to the infinite matrix issue from a computational perspective, the truncation leads to some important mathematical questions

1. Is the truncated matrix invertable?

2. If the truncated matrix is invertable, does the finite version converge to the actual solution?

3. If the finite version of the matrix converges to the actual solution, what is the convergence rate?

These very important questions must be answered to have some reasonable level of trust in the solution method. The problem is how to answer such questions about the truncation of the infinite matrix. Infinite linear systems are an uncommon occurrence in computational and applied mathematics. Direct analysis of the system proved difficult and essentially hopeless. The only recourse was to reexamine the problem from a more rigorous and well understood approach and try to draw some parallels. Such an approach is the variational formulation.

2.6 Variational Formulation

The variational or weak form of differential equations is the cornerstone of the modern theory of elliptic differential equations. The variational approach not only provides a basis for mathematical proofs of existence and uniqueness, but also provides a basis for robust numerical methods including the finite element method. We will look for a unique weak solution of the Laplace equation with boundary conditions in an appropriate space of functions. It will be shown that the variational method provides the necessary avenue to analyze the Fourier solution method.

For the variational formulation first define the solution domain. Place an artificial boundary in the gap at y=0 and y=b. The domain S is shown in the figure 2.7.

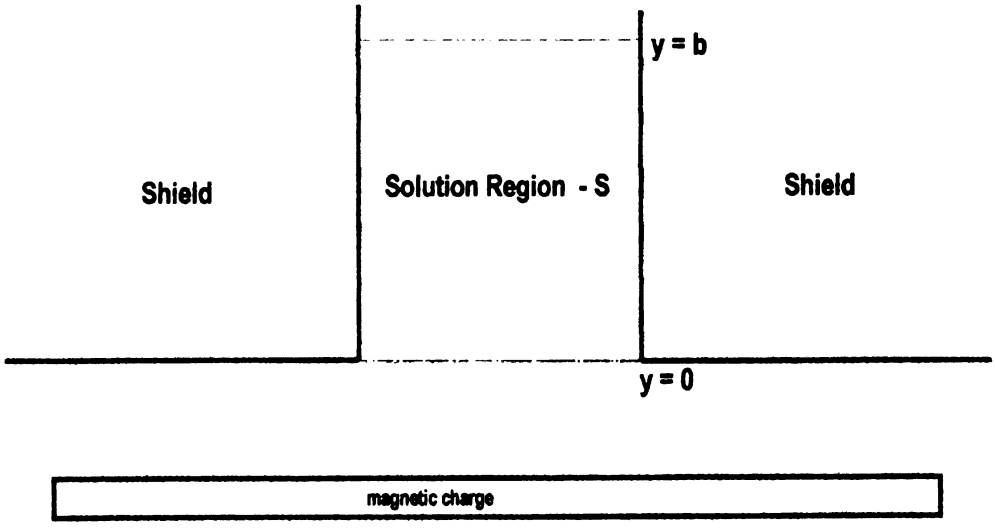

Figure 2.7. Diagram of solution S domain for the variational problem

We will now look for a solution in the rectangular region S from $x = 0$ to $x = G_s$

and $y = 0$ to $y = b$. Note that Γ will denote the boundary of S.

To enforce that $u(0, y) = u(G_s, y) = 0$, we will look for the solution in the space of functions

$$\widetilde{H}_0^1(S) = \left\{ w \in H^1(S) \mid w(0, y) = u(G_s, y) = 0 \right\} \tag{2.22}$$

The weak form of the problem is constructed as follows:

1.Multiply both sides of the equation by a function w in $\widetilde{H}_0^1(S)$

$$\int_S \triangle u w = 0 \tag{2.23}$$

2. Apply integration by parts

$$-\int_s \nabla u \cdot \nabla w + \int_\Gamma \frac{\partial u}{\partial n} w = 0 \tag{2.24}$$

Before moving on to the variational solution, we must examine the boundary term of the weak form of the equation. The boundary conditions must be carefully constructed for the interface between region I and region II as well as to truncate the region I domain to be finite.

We know that $w(0, y) = w(G_s, y) = 0$, but we must also specify boundary conditions on $\Gamma_1(y = b)$ and $\Gamma_2(y = 0)$. First, on Γ_1 we know the solution will be of the form

$$u = \sum_{n=1}^{\infty} A_n \sin\left(\frac{n\pi x}{G_s}\right) \mathrm{e}^{-\left(\frac{n\pi}{G_s}\right)y} \tag{2.25}$$

Therefore, on Γ_1 we have

$$\frac{\partial u}{\partial n} = \frac{\partial u}{\partial y} = \sum_{n=1}^{\infty} \left(\frac{-n\pi}{G_s}\right) A_n \sin\left(\frac{n\pi x}{G_s}\right) \mathrm{e}^{-\left(\frac{n\pi}{G_s}\right)b} \tag{2.26}$$

Hence, a Dirichlet to Neuamn map $T_1(u)$ can be defined on Γ_1 by,

$$\frac{\partial u}{\partial n} = T_1(u) = \sum_{n=1}^{\infty} \left(\frac{-n\pi}{G_s}\right) A_n \sin\left(\frac{n\pi x}{G_s}\right) \mathrm{e}^{-(\frac{n\pi}{G_s})b} \tag{2.27}$$

On the boundary Γ_2, we must refer back to the second matching condition:

$$\frac{\partial u}{\partial y} = \mathcal{F}_x^{-1}(-\kappa B + \kappa C) \tag{2.28}$$

Again solve (2.11) for C and substitute into the previous equation to get

$$\frac{\partial u}{\partial y} = \mathcal{F}_x^{-1}(-2\kappa B + \kappa \mathcal{F}_x(u)) \tag{2.29}$$

or

$$\frac{\partial u}{\partial y} = \mathcal{F}_x^{-1}(\kappa \mathcal{F}_x(u)) + g \tag{2.30}$$

where $g = -2\mathcal{F}_x^{-1}(\kappa B)$.

Hence, a Dirichlet to Neuman map $T_2(u)$ can be defined on Γ_2 as the following:

$$\frac{\partial u}{\partial n} = T_2(u) + g = -\mathcal{F}_x^{-1}(\kappa \mathcal{F}_x(u)) - g \tag{2.31}$$

Now, put the maps $T_1(u)$ and $T_2(u)$ into the weak form of the equation (2.24)

$$-\int_s \nabla u \cdot \nabla w + \int_{\Gamma_1} T_1(u) w + \int_{\Gamma_2} T_2(u) w = \int_{\Gamma_1} g w \tag{2.32}$$

The weak form of the equation defines a bilinear form

$$a(u, w) = -\int_s \nabla u \cdot \nabla w + \int_{\Gamma_1} T_1(u) w + \int_{\Gamma_2} T_2(u) w \tag{2.33}$$

and a bounded linear functional

$$\langle g, w \rangle = \int_{\Gamma_1} gw \tag{2.34}$$

The solution of the variational form of the problem is a function $u \in \widetilde{H}_0^1(S)$ such that

$$a(u, v) = \langle g, v \rangle \tag{2.35}$$

for all $v \in \widetilde{H}_0^1(S)$.

2.7 Existence and Uniqueness of Variational Solution

The weak or variational formulation is very useful for proving existence and uniqueness of the problem at hand. The established theory for elliptic differential equations can be used here as in the following theorem.

Theorem 2.1 *The variational problem 2.35 has a unique solution in* $\widetilde{H}_0^1$.

PROOF. First, it must be shown $a(u, v)$ is continuous bilinear form on $\widetilde{H}_0^1(S)$ that is to say

$$a(u, v) \leq C\|u\|_{\widetilde{H}_0^1(S)}\|v\|_{\widetilde{H}_0^1(S)} \tag{2.36}$$

Next, we must establish coercivity of the bilinear form which means

$$a(u, u) \geq C\|u\|^2_{\widetilde{H}_0^1(S)} \tag{2.37}$$

Using the previous two facts we apply the Lax-Milgram Lemma to establish that there exists a unique solution to the differential equation in $\widetilde{H}_0^1(S)$.

Now, we will establish the continuity of $a(u,v)$. Using the Cauchy-Schwartz inequality we have

$$\int_s \nabla\phi \cdot \nabla v \leq C\|u\|\|v\| \tag{2.38}$$

By orthogonality, the Cauchy-Schwartz Inequality and the Trace Theorem we have

$$\int_{\Gamma_1} T_1(u)v = \sum_{n=1}^{\infty} \frac{n\pi}{G_s} A_n B_n \leq C\|u\|\|v\|. \tag{2.39}$$

Now, by Parsveval's Theorem, Cauchy-Schwartz inequality and the Trace Theorem.

$$\int_{\Gamma_2} T_2(u)v = \int_{-\infty}^{+\infty} \kappa \mathcal{F}_x(u)\mathcal{F}_x^{-1}(u) \leq C\|u\|\|v\| \tag{2.40}$$

Thus, we have continuity

$$a(u,v) \leq C\|u\|\|v\| \tag{2.41}$$

Now, prove the coercivity of the bilinear form $a(u,v)$:

$$-a(u,u) = \int_S \nabla u^2 + \sum_{n=1}^{\infty} \frac{n\pi}{G_s} {A_n}^2 + \int_{-\infty}^{+\infty} \kappa \mathcal{F}_x(u)^2 \tag{2.42}$$

Poincaré's inequality tells us that

$$\int_S \nabla u^2 \geq C\|u\|^2 \tag{2.43}$$

Since the other two terms are clearly positive, we have the result:

$$a(u,u) \geq C\|u\|^2 \tag{2.44}$$

Therefore, the conditions of Lax-Milgram Lemma are satisfied, and we are guaranteed the existence of a unique solution $u \in \widetilde{H}_0^1(S)$

2.8 Fourier Method Versus the Variational Formulation

2.8.1 Existence of the Fourier Method Solution

The connection between the Fourier series method and the variational formulation can be found by considering subspaces of $\widetilde{H}_0^1(S)$ If a space V_N is a subspace of $\widetilde{H}_0^1(S)$ then there is a unique solution to the variational problem over the subspace as well because continuity and coercivity apply on the subspace the same as on the entire space. Using this idea, and theorem 2.1 we want to try find some parallel between the Fourier solution method and the variational form. The first conclusion that can be drawn is that the truncated matrix from the Fourier method is invertible. We will see that this fact is just a simple corollary of the uniqueness result for the variational problem.

Note that there is a unique solution to

$$a(u_N, v_N) = \langle g, v_N \rangle \tag{2.45}$$

with $u_n \in V_N$. The question is how can we use this notion to relate the variational formulation to that of the Fourier method?

In order to make the connection from the variational formulation to the Fourier method first define

$$V_N = \left\{ u_N \in \widetilde{H}_0^1(S) \mid u_N = \sum_{n=1}^{N} A_n \sin\left(\frac{n\pi x}{G_s}\right) \mathrm{e}^{\left(\frac{-n\pi}{G_s}\right)y} \right\} \tag{2.46}$$

which is a finite dimensional subspace, hence there is a unique solution to the variational problem in this space.

If we examine the variational form of the problem when the functions come from the subspace V_N, the connection can be made. Let us solve the variational form of the problem in V_N using the Galerkin method. Let $v_m = \sin\left(\frac{m\pi}{G_s}\right) e^{\left(\frac{-m\pi}{G_s}\right)y}$ and carry out some calculations.

$$\begin{aligned} -\int_s \nabla u_N \cdot \nabla v_m &= \int_0^b \frac{2}{G_s}\left(\frac{m\pi}{G_s}\right) A_m e^{\left(\frac{-m\pi}{G_s}\right)y} \\ &= \left[\left(\frac{m\pi}{G_s}\right)\left(\frac{2}{G_s}\right) A_m e^{\left(\frac{-2m\pi}{G_s}\right)b} \right. \\ &\quad \left. -\left(\frac{m\pi}{G_s}\right)\left(\frac{2}{G_s}\right) A_m\right] \end{aligned}$$

$$\begin{aligned} \int_{\Gamma_1} T_1(u_N) v_m &= \int_0^{G_s} \left[\sum_{n=1}^{N} -\left(\frac{n\pi}{G_s}\right) A_n \sin\left(\frac{n\pi x}{G_s}\right) \cdot \right. \\ &\quad \left. e^{\left(\frac{-n\pi}{G_s}\right)b}\right] \sin\left(\frac{m\pi x}{G_s}\right) e^{\left(\frac{-m\pi}{G_s}\right)b} \\ &= -\left(\frac{m\pi}{G_s}\right)\left(\frac{2}{G_s}\right) A_m e^{\left(\frac{-2m\pi}{G_s}\right)b} \end{aligned}$$

$$\begin{aligned} \int_{\Gamma_2} T_2(u_N) v_m &= -\int_0^{G_s} \mathcal{F}_x^{-1}(\kappa \mathcal{F}_x(u_N)) \sin\left(\frac{m\pi x}{G_s}\right) \\ &= \int_{-\infty}^{\infty} \kappa \mathcal{F}_x(u_N) \mathcal{F}_x^{-1}\left(\sin\left(\frac{m\pi x}{G_s}\right)\right) \end{aligned}$$

Continuing with the last integral

$$\int_{-\infty}^{\infty} \mathcal{F}_x(u_N)\mathcal{F}_x^{-1}\left(\sin\left(\frac{m\pi x}{G_s}\right)\right) = \sum_{n=1}^{N}\int_{-\infty}^{\infty} A_n\mathcal{F}_x\left(\sin\left(\frac{n\pi x}{G_s}\right)\right)\mathcal{F}_x^{-1}\left(\sin\left(\frac{m\pi x}{G_s}\right)\right) \quad (2.47)$$

Notice that this last expression is exactly

$$-\sum_{n=1}^{N} K_{nm}A_n \quad (2.48)$$

Putting all the integrations together we get:

$$a(u_N, v_m) = -\left(\frac{m\pi}{G_s}\right)\left(\frac{2}{G_s}\right)A_m - \sum_{n=1}^{N} K_{nm}A_n \quad (2.49)$$

Also, note that

$$\langle g, v_m\rangle = -\int_{-\infty}^{\infty} 2B\mathcal{F}_x^{-1}\left(\sin\left(\frac{m\pi x}{G_s}\right)\right) \quad (2.50)$$

Which is exactly $-B_m$ from the Fourier method. Therefore, we see now that solving the variational problem with the galerkin method

$$a(u_N, v_N) = \langle g, v_N\rangle \quad (2.51)$$

produces the exact same matrix as the truncated matrix from the Fourier method.

$$\widetilde{K_N}\left\{\overline{A_N}\right\} = \left\{\overline{B_N}\right\} \quad (2.52)$$

Now we can answer the first question about the Fourier method. The truncated

matrix is invertible since the variational form has a unique solution in V_N.

2.8.2 Convergence of Fourier Method Solution

We can use analysis of the variational formulation on the subspace V_N to determine the convergence properties of the Fourier Series method.

Theorem 2.2 *The Fourier series method converges to the true solution of the problem in $\widetilde{H}_0^1$ with convergence rate N^{-1}.*

PROOF. Cea's Lemma [20] states that the solution to the variational problem in V_N is the best possible approximation of the true solution u in $\widetilde{H}_0^1$.

$$\|u - u_n\| \leq C \left(\inf_{\widetilde{u} \in V_N} \|u - \widetilde{u}\| \right) \tag{2.53}$$

This lemma is enough to answer the second question about the Fourier method. By letting $N \to \infty$ we see that the finite Fourier method will converge to the actual solution.

Also, Cea's lemma allows us to answer the third question about the Fourier method regarding the convergence rate. We just need to determine the best approximation of u possible in the space V_N under the norm $H_1(S)$.

It can be shown that the approximations u_N will converge to the actual series solution of u

$$u = \sum_{n=1}^{\infty} A_n \sin\left(\frac{n\pi x}{G_s}\right) \mathrm{e}^{\left(\frac{-n\pi}{G_s}\right)y} \tag{2.54}$$

with error of order N^{-1} in $H_1(S)$. The key to proving this is to show that the trace of the first derivatives of u are actually integrable on the boundary Γ_2. The trace theorem alone does not give this fact. Some examination of the solution near the

corners of the shields is necessary[28][18]. Therefore, we can conclude that

$$\|u - u_n\|_{H_1(S)} \leq \frac{C}{N} \tag{2.55}$$

Thus the last question is answered since we have a convergence rate. Hence we know u and $H = \nabla u$ will converge with order N^{-1}.

2.9 Finite Element Formulation

An alternative method for solving this problem would be a finite element method (FEM). Although [24] claims that the FEM would not be practical here, we can actually see that the above analysis of the variational form shows that the FEM may actually be quite feasible. Beyond that, it may be more useful since we can deal with the inhomogeneous problem as well. In addition, using the finite element method, it is much easier to do computations for related problems such as the finding the field in the gap with a charge in the gap as well. In micromagnetics, this is known as the demagnetizing field. Also, if necessary, a non-uniform mesh can be used to deal with innaccuracies due to singularities at the corners of the gap interface.

2.10 Numerical Examples

Here we will give some demonstrations of the Fourier series method at work. Examples will be given in two and three dimensional situations. Also, an example will be shown where the field in the gap region due to a charge in the gap region is computed using the finite element method.

The charge distribution will be a model of the transition from one sector to a

second sector. The magnetization is

$$M(x - x_0) = M_r \vec{x} \cdot \begin{cases} -1 & : \quad x \leq x_0 \\ \\ +1 & : \quad x > x_0 \end{cases}. \tag{2.56}$$

M_r is the magnitude of the magnetization and $\vec{x}$ is the unit vector in the x-direction. Since the magnetization is a step function, the the magnetic charge is given by

$$\rho_m = \nabla \cdot M(x - x_0) = 2M_r \delta(x - x_0). \tag{2.57}$$

Using this charge and the appropriate Green's function, the media field can be computed.

2.10.1 Two-dimensional Fourier Method

The first examples will illustrate the Fourier series method in two dimensions. The potential and both field components of the magnetic fields will be given.

2.10.2 Three-dimensional Fourier method

The Fourier series method can also be applied in three dimensions as well. The only additional computation is taking the Fourier transform in the z-direction. The magnetization in this situation is the same as the two-dimensional case except that it has a finite support in the z-direction. Although the rigorous analysis is not given for the three-dimensional case, it is a very efficient way to compute a three-dimensional magnetic field.

2.10.3 Finite element computation

The MR film has its own magnetization distribution. Hence, it is often of interest to compute the so-called demagnetizing field of the MR film. In terms of the problem, this is computing the magnetic field in the gap (region I) due to a charge in the gap as well. The Fourier method is not as forthcoming in this case. Also, if one wants to account for the inhomgenous material which the MR-film is made of, a more general method is necessary. The solution is the use of the finite element method. Here quasi-linear elements were used to compute the potential inside the gap due to a charge which is inside the gap. The charge distribution in the experiment is just a constant charge distribution with a thin support in the middle of the gap spacing. The charge distribution simulates a MR film which has its own magnetic charge.

2.10.4 Field Below the Gap (Region II)

The same theory allows the computation of the field outside the gap below the shields. The field outside the gap is known as the image field. Once the Fourier method has been used to compute the Fourier coefficients A_n, the only unknown in the equation 2.10 is the Fourier transform C. This can be determined and inserted into equation 2.4 to compute the field below the gap in region II.

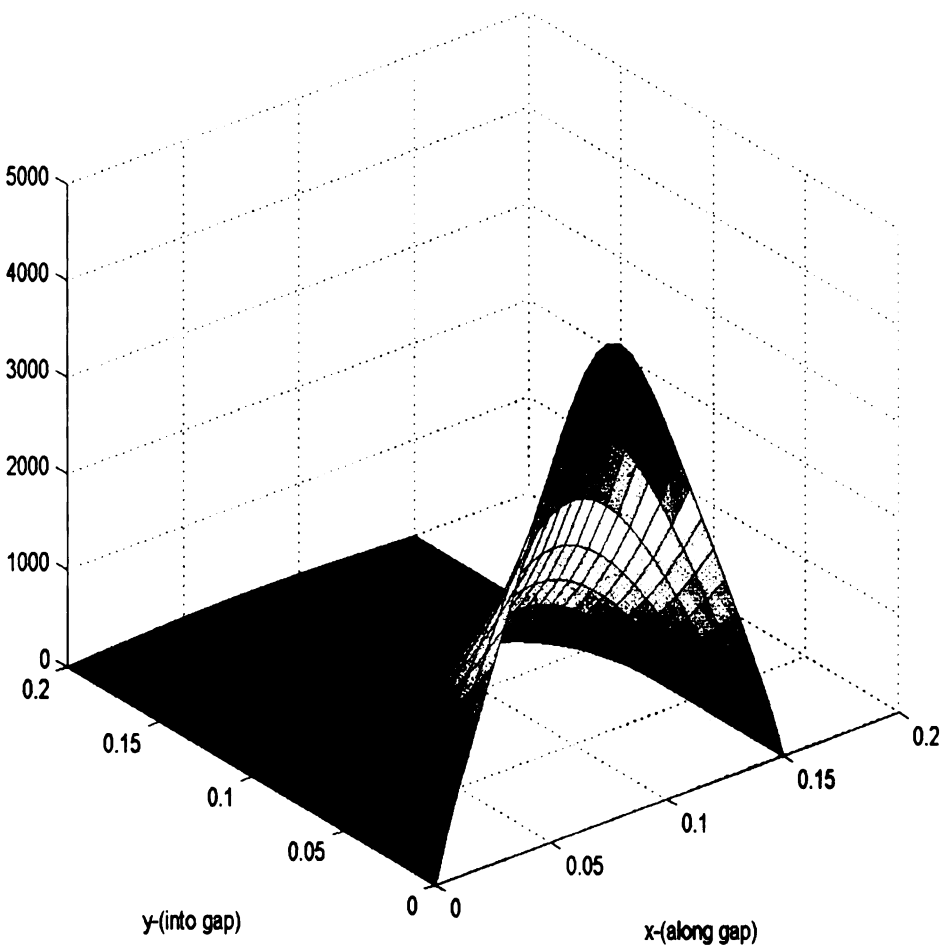

Figure 2.8. The magnetic potential inside the gap.

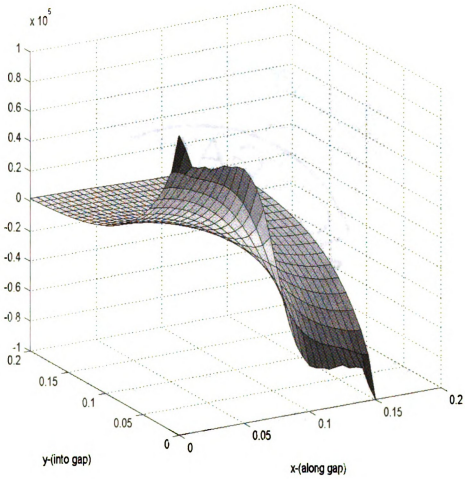

Figure 2.9. The x component of the magnetic field inside the gap.

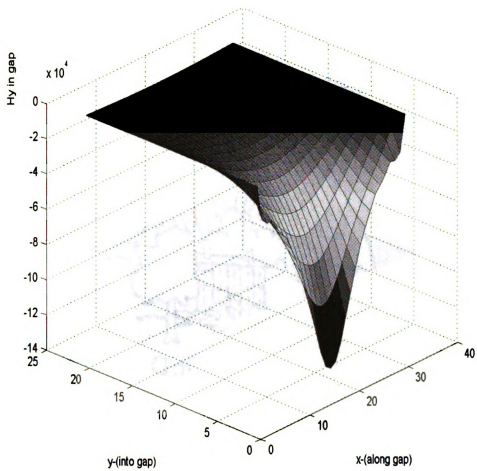

Figure 2.10. The y component of the magnetic field inside the gap.

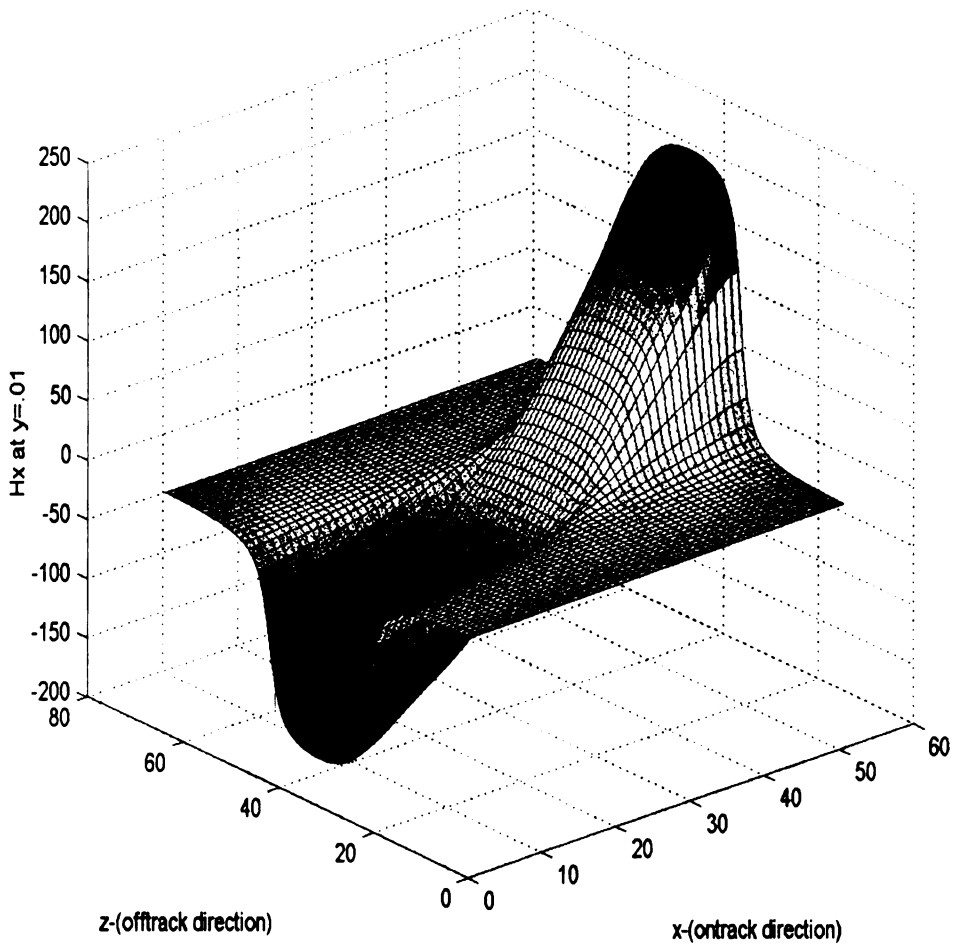

Figure 2.11. The x component of the magnetic field .01 micrometers within the gap

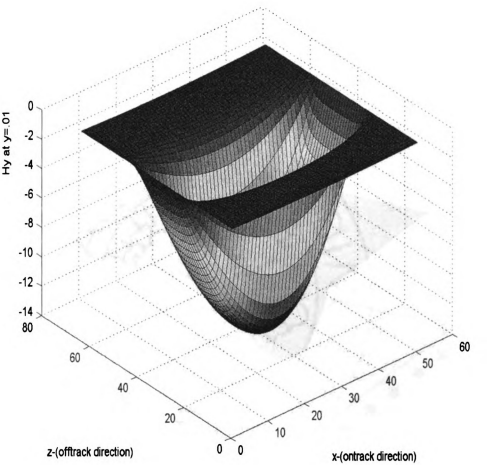

Figure 2.12. The y component of the magnetic field .01 micrometers into gap

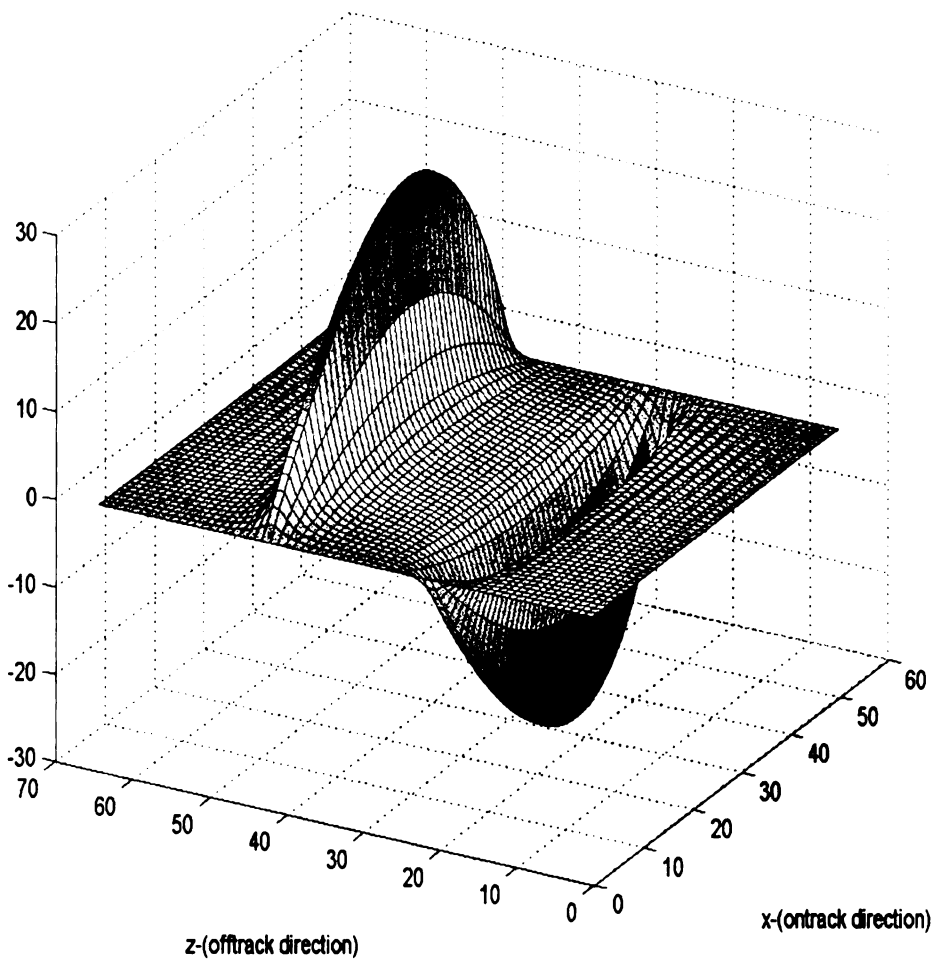

Figure 2.13. The z component of the magnetic field .01 micrometers into gap.

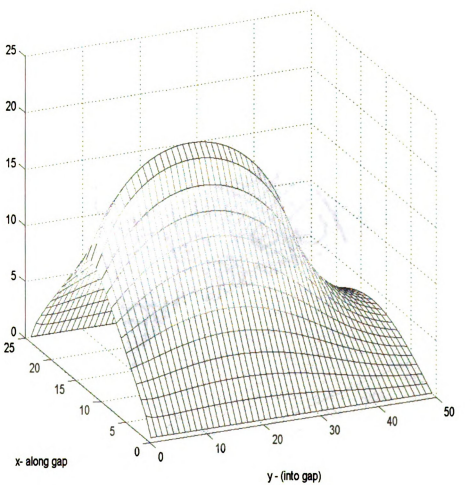

Figure 2.14. Potential from charge inside the gap using finite element method.

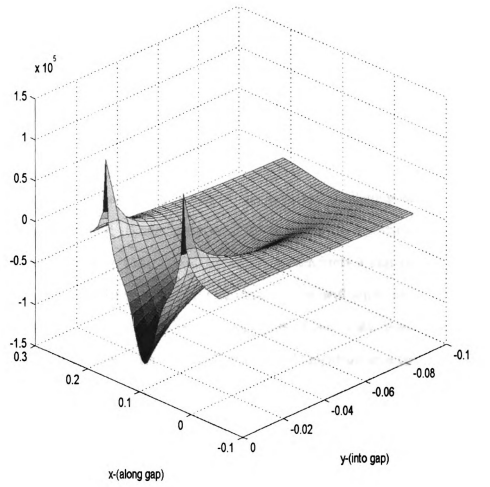

Figure 2.15. The y-component of the magnetic field outside the gap.

CHAPTER 3

Inverse Point Source Problem

3.1 Introduction

Understanding the human brain is one of the greatest challenges still faced by scientists in modern times. Since brain activity is based on electrical interactions of neurons, it is no surprise that the study of electromagnetics can play a role in the understanding of neural behavior. In this chapter, we will show an example of how the Maxwell's equations can help in the treatment of the brain disease epilepsy.

Much research has been done in the field of dipole location in a conducting media. Unfortunatley, almost without exception, the methods are iterative least-squares fitting algorithms which tend to be unstable. Also, the methods rely on a quasi-static model of the dipole current, which while not an unreasonable approximation, provides an unknown amount of error into the process [21][12]. Since the most reasonable *a priori* assumption is that the fields are low frequency, it is desirable from a mathematical perspective to find a method for which the accuracy depends asymptotically on the frequency [4]. That is to say, we want the error to be controlled by the magnitude of the frequency.

3.2 Problem Description

Here the problem will be described. Also, preliminary issues such as existence and uniqueness of the direct problem will be summarized. Let (x_1, x_2, x_3) be the Cartesian coordinate system equipped with an orthonormal basis (e_1, e_2, e_3). Let Ω^i be a bounded smooth domain in $\mathbb{R}^3$ with boundary Γ. Let Ω^e be the complement of $\overline{\Omega^i}$ in $\mathbb{R}^3$. We assume that Γ is of class $\mathcal{C}^{2,\alpha}$ for $0 < \alpha < 1$ and denote by n its unit outward normal.

We consider the propagation of time-harmonic electromagnetic waves in an inhomogeneous dielectric medium Ω^i with electric permittivity ε, magnetic permeability μ, and electric conductivity σ. Assume that ε, μ and σ are real valued bounded functions which satisfy $\Re e\, \varepsilon \geq \varepsilon_i > 0$, $\Re e\, \mu \geq \mu_i > 0$ and $\sigma \geq \sigma_i > 0$ in Ω^i, where ε_i, μ_i and σ_i are real positive constants. The functions ε and σ are also assumed to be of class $\mathcal{C}^{1,\alpha}$ in $\overline{\Omega^i}$ and μ is assumed to be of class $\mathcal{C}^{2,\alpha}$. Assume further that the exterior domain Ω^e is homogeneous with electric permittivity ε_0, magnetic permeability μ_0, and zero conductivity.

With the dielectric material Ω^i containing an electric dipole, the wave propagation is governed by Maxwell equations:

$$\nabla \times E = -i\omega\,\mu\, H \quad \text{in } \mathbb{R}^3, \tag{3.1}$$

$$\nabla \times H = i\omega\,\varepsilon\, E - \sigma\, E + \delta(x - x_0)\, p_0 \quad \text{in } \mathbb{R}^3, \tag{3.2}$$

together with the Silver-Müller radiation condition

$$\lim_{|x| \to +\infty} |x| \Big(\sqrt{\mu_0}\, H \times \frac{x}{|x|} - \sqrt{\varepsilon_0}\, E \Big) = 0\,. \tag{3.3}$$

Here $\delta(x - x_0)$ is the Dirac function at the point x_0 (the source point) and p_0 (the direction of the electric dipole) is a constant vector.

Given the source point x_0 and the direction of the electric dipole p_0, the direct problem is to determine the field distributions E, H for a fixed frequency ω, and fixed material functions ε, μ, and σ.

Concerning the direct problem, the following existence, uniqueness and regularity results hold [4].

Lemma 3.1 *The system of Maxwell's equations (3.1-3.3) attains a unique solution. Moreover, the solution* (E, H) *is in* $\mathcal{C}^{2,\alpha}(\Omega^i \setminus \{x_0\} \cup \Omega^e)$.

Our goal is to study the inverse source problem, *i.e.*, to determine the point source x_0 and the direction vector p_0 from boundary measurements of the tangential components of the electric field E and the magnetic field H on the boundary Γ of Ω^i. We assume that x_0 belongs to the interior domain Ω^i, i.e., x_0 doesn't lie on the boundary Γ of Ω^i. In the following, we will establish uniqueness and stability of the inverse problem, and present a reconstruction method based on a low frequency asymptotic analysis of the model problem.

3.3 Uniqueness of the Inverse Problem

Here we review the issue of uniqueness of the inverse problem. The question is whether or not measurements of the tangential components of the electric and magnetic fields on the boundary of the conducting volume will uniquely determine the location and orientation of the dipole current. The answer to the question is in the following theorem [4].

Theorem 3.1 *Let* x_0 *and* x_1 *be two source points in* Ω^i *and* p_0 *and* p_1 *be two constants vectors. Assume that* (E_j, H_j) *for* $j = 0, 1$ *are the corresponding solutions of Maxwell's*

equations:

$$\begin{cases} \nabla\times E_j \;=\; -i\omega\,\mu\,H_j \quad \text{in } \mathbb{R}^3, \\ \nabla\times H_j \;=\; i\omega\,\varepsilon\;E_j - \sigma\,E_j + \delta(x-x_j)\,p_j \quad \text{in } \mathbb{R}^3, \\ \lim\limits_{|x|\to+\infty} |x|\Big(\sqrt{\mu_0}\,H_j \times \dfrac{x}{|x|} - \sqrt{\varepsilon_0}\,E_j\Big) \;=\; 0. \end{cases}$$

If $E_0 \times n|_\Gamma = E_1 \times n|_\Gamma$ *or* $H_0 \times n|_\Gamma = H_1 \times n|_\Gamma$ *then* $x_0 = x_1$ *and* $p_0 = p_1$.

Clearly the theorem states that the same tangential components of the fields can only be produced by the same dipole current.

3.4 Inverse Problem Method

By eliminating the magnetic field H in the Maxwell equations (3.1), (3.2), we have

$$\nabla\times\frac{1}{\mu}\nabla\times E - (\omega^2\varepsilon + i\omega\sigma)E = \delta(x-x_0)\,p_0 \quad \text{in } \mathbb{R}^3. \tag{3.4}$$

Introduce an operator

$$\mathcal{M}_\omega(e) = \nabla\times\frac{1}{\mu}\nabla\times e - \omega^2\,\varepsilon\,e - i\omega\,\sigma\,e\,.$$

Define the kernel of $\mathcal{M}_\omega$ to be

$$\mathcal{N}(\mathcal{M}_\omega,\Omega^i) = \Big\{u \in (\mathcal{C}^{2,\alpha}(\overline{\Omega^i}))^3, \mathcal{M}_\omega(u) = 0 \text{ in } \Omega^i\Big\}.$$

Multiplying (3.4) by $e \in \mathcal{N}(\mathcal{M}_\omega,\Omega^i)$ and integrating by parts lead to the following identity

$$p_0\,.\,e(x_0) = -\frac{i}{\omega}\int_\Gamma \frac{1}{\mu}\nabla\times E \times n\,.\,e + \frac{i}{\omega}\int_\Gamma \frac{1}{\mu}\nabla\times e\,.\,E\times n. \tag{3.5}$$

The identity (3.5) plays a crucial role in our analysis of the inverse problem.

In this section, we introduce a reconstruction method for solving the inverse problem. From now on, we make some general assumptions:

- the frequency ω is small;
- the conductivity function σ is a fixed constant in Ω^i.

The first assumption is essential for our asymptotic analysis of the inverse problem. The second assumption is a technical one. We will show that similar results may be established for a variable conductivity σ.

We next describe a method for solving the inverse problem. Our main idea is to construct asymptotic solutions to $\mathcal{M}_\omega(u) = 0$ in Ω^i when the frequency ω goes to zero. The identity (3.5) plays an important role in the identification of the source point x_0 and the direction vector p_0. A crucial step of our method is to construct special approximate solutions of the kernel $\mathcal{N}(\mathcal{M}_\omega, \Omega^i)$.

Let $\varphi^{(0)}$ be a scalar harmonic function in Ω^i of class $\mathcal{C}^{2,\alpha}$ and $u^{(1)}$ be a solution of

$$\nabla \times \frac{1}{\mu} \nabla \times u^{(1)} = i\sigma \nabla \varphi^{(0)} \quad \text{in } \Omega^i.$$

It is easily seen that

$$\mathcal{M}_\omega \Big[\nabla \varphi^{(0)} + \omega u^{(1)} \Big] = 0(\omega^2) \quad \text{in } \Omega^i,$$

which implies by using (3.5) that

$$p_0 \,.\, \nabla \varphi^{(0)}(x_0) = \int_\Gamma H \times n \,.\, \nabla \varphi^{(0)} + i \int_\Gamma \frac{1}{\mu} \nabla \times u^{(1)} \,.\, E \times n + 0(\omega).$$

We now make the following special choices of harmonic functions in Ω^i: x_1, x_2, x_3, and $e^{i\xi \cdot x}$, where $\xi \in \mathbb{C}^3$ is such that $\xi \,.\, \xi = 0$. The first three harmonic functions allow us

to determine approximately the vector p_0 up to an error of order ω; while the fourth function with three different values of ξ determines the point x_0 up an error of order ω.

More precisely, let ${p_0}^{(1)}$ and ${x_0}^{(1)}$ be defined by

$$ {p_0}^{(1)} \cdot e_j = \int_\Gamma H \times n \cdot e_j + i \int_\Gamma \frac{1}{\mu} \nabla \times u_j^{(1)} \cdot E \times n \,, \tag{3.6} $$

$$ {p_0}^{(1)} \cdot \xi_j \, e^{i\xi_j \cdot {x_0}^{(1)}} = \int_\Gamma H \times n \cdot \xi_j \, e^{i\xi_j \cdot x} \quad + i \int_\Gamma \frac{1}{\mu} \nabla \times v_j^{(1)} \cdot E \times n \,, \tag{3.7} $$

where $\xi_j \in \mathbb{C}^3$ for $j = 1, 2, 3$ are three different complex constants that satisfy $\xi_j \cdot \xi_j = 0$. The functions $u_j^{(1)}$ and $v_j^{(1)}$ are solutions of the following problems

$$ \nabla \times \frac{1}{\mu} \nabla \times u_j^{(1)} = i\sigma \, e_j \tag{3.8} $$

and

$$ \nabla \times \frac{1}{\mu} \nabla \times v_j^{(1)} = i\sigma \, \xi_j e^{i\xi_j \cdot x} \quad \text{in } \Omega^i. \tag{3.9} $$

The above analysis gives rise to a simple numerical method for determining the source point x_0 and the direction vector p_0. From the knowledge of the values of $H \times n$ and $E \times n$ in a finite number of points on Γ, where the wavelength $\lambda = 2\pi/\omega$ is large compared to the characteristic size of Ω^i. We first compute $u_j^{(1)}$ and $v_j^{(1)}$ by solving the equations (3.8) and (3.9), respectively. We then interpolate the integrals involving in formula (3.6) to a precision of order ω ($\sim 10^{-2}$).

We next present convergence properties of the method.

Theorem 3.2 *Assume that E and H are solutions of the Maxwell equations (3.1-*

3.3). Let ${p_0}^{(1)}$ *and* ${x_0}^{(1)}$ *satisfy*

$$ {p_0}^{(1)} \cdot e({x_0}^{(1)}) = \int_\Gamma H \times n \cdot e + \frac{i}{\omega} \int_\Gamma \frac{1}{\mu} \nabla \times e \cdot E \times n + 0(\omega), $$

for any e *in* $\mathcal{N}(\mathcal{M}_\omega, \Omega^i)$. *Then*

$$ |{p_0}^{(1)} - p_0| = 0(\omega) \text{ and } |{x_0}^{(1)} - x_0| = 0(\omega). $$

Finally, from the stability result the following holds.

Corollary 3.1 *The following estimates hold [4]*

$$ |{p_0}^{(1)} - p_0| = 0(\omega) \text{ and } |{x_0}^{(1)} - x_0| = 0(\omega), $$

where ${p_0}^{(1)}$ *and* ${x_0}^{(1)}$ *are determined from (3.6) and (3.7).*

Corollary 3.2 *If* E *satisfies the Maxwell equations (3.1-3.3) together with the identity*

$$ -\frac{i}{\omega} \int_\Gamma \frac{1}{\mu} \nabla \times E \times n \cdot e + \frac{i}{\omega} \int_\Gamma \frac{1}{\mu} \nabla \times e \cdot E \times n = p_1 \cdot e(x_1), $$

for any $e \in \mathcal{N}(\mathcal{M}_\omega, \Omega^i)$, *then*

$$ x_1 = x_0 \quad \text{and} \quad p_1 = p_0. $$

The method can also be applied to variable conductivities with some slight variation. The variable conductivity case is very important since different regions in the human head have significant differences in conductivity. For example the conductivity of the skull is two orders of magnitude less than that of the gray matter. In the

case that the conductivity σ is a variable function in Ω^i, the situation becomes more complicated. We study this general case by modifying our approach.

Construct a solution $u^{(1)}$ satisfying

$$\nabla \times \frac{1}{\mu} \nabla \times u^{(1)} = i\sigma \nabla \varphi \text{ in } \Omega^i .$$

However, since σ is no longer a constant, the function φ can not be a harmonic function. In fact, from our previous discussion, it is not difficult to see that the function φ should be chosen to solve

$$\nabla \cdot (\sigma \nabla \varphi) = 0 .$$

3.5 Computation of Sample Data Through the Direct Problem

As we can see from the description of the inverse method, the input into the inverse problem is tangential electric and magnetic fields measured on the boundary of a conducting region. Verification and testing of the method requires producing some data which can be used as sample input. Unfortunately, computation of low frequency dipole fields in an open region is not a simple task. One is confronted with many numerical issues. For instance, due to the nature of the dipole source, the solution will be singular. Since we are interested in boundary measurements relatively close to the singularity, the error introduced computationally is a significant factor. Also, to solve the problem in an open domain requires the use of some sort of artificial or transparent boundary conditions. While there are many ways to deal with this issue, most will have error based on the distance of the boundary from the source in terms of wavelength. Due to the very long wavelengths one encounters in the low

frequency problem, this is another issue which creates difficulty. However, while the possibilities for computation are limited, there are some methods which can be used to create some direct problem data

3.5.1 Green's Function

The Green's function method is the ideal method to compute the electric and magnetic field when all of the material parameters are constant in an infinite medium. Consider a dipole current source of the form

$$J(x) = \delta(x - x_0)p_0 \tag{3.10}$$

where x_0 is the position of the dipole, and p_0 is the orientation vector. The experiment will determine the location and orientation of the dipole current within a fictitious sphere using the tangential electric and magnetic field components measured on the sphere's surface.

The computation of the electric an magnetic fields due to a dipole current source in the geometry described above is done with the use of an appropriate Green's function. The vector Green's function must satisfy the following differential equation

$$\nabla \times \nabla \times G - k^2 G = I\delta(x - x_0). \tag{3.11}$$

along with the radiation boundary condition at infinity. The solution of (3.11) can be written as

$$G(x, x') = \left[I + \frac{1}{k^2} \nabla \nabla \cdot \right] g(x, x') \tag{3.12}$$

where g is the scalar Green's function

$$g(x,x') = \frac{e^{ik|x-x'|}}{4\pi|x-x'|}. \tag{3.13}$$

Therefore, given the current distribution $J(x)$, the electric field external to any volume V containing the current distribution is given by an integration over V with respect to the primed variable

$$E(x) = i\omega\mu \left[I + \frac{1}{k^2} \nabla \nabla \cdot \right] \int_{V'} g(x,x') J(x'). \tag{3.14}$$

In particular, since the current source considered here is a dipole as shown in (3.10) the electric field is

$$E(x) = i\omega\mu \left[I + \frac{1}{k^2} \nabla \nabla \cdot \right] g(x,x_0) p_0. \tag{3.15}$$

Further the magnetic field is given by

$$H(x) = \frac{1}{i\omega\mu} \nabla \times E(x). \tag{3.16}$$

For more details on the vector Green's function see [27].

3.5.2 Born Approximation

A slightly more realistic geometry can be modeled if one incorporates the Born approximation [17]. Suppose the conductivity is a function $\sigma(x) = \sigma + \sigma_1(x)$.

$$\nabla \times \frac{1}{\mu} \nabla \times E - (\omega^2 \varepsilon + i\omega(\sigma + \sigma_1(x)))E = \delta(x - x_0)\, p_0 \quad \text{in } \mathbb{R}^3. \tag{3.17}$$

or

$$\nabla\times\frac{1}{\mu}\nabla\times E-(\omega^2\varepsilon+i\omega\sigma)E=\delta(x-x_0)\,p_0+Q(x)E\quad\text{in }\mathbb{R}^3. \tag{3.18}$$

where $Q(x)=-i\omega\sigma_1(x)$ and V_1 is the support of $Q(x)$.

Using the Green's function, the solution is of the form

$$E=E^0+\int_{V_1}G\cdot Q(x)E. \tag{3.19}$$

The E^0 is the field in the homogeneous region and the second term is the scattered field due to the change in conductivity. The second term on the right hand side of 3.19 will be denoted as E^1 which is the scattered field due to the obstacle. The Born approximation is a first order approximation of the scattered field [17]

$$E^1=\int_{V_1}G\cdot Q(x)E^0 \tag{3.20}$$

3.5.3 Quasi-static approximation

Even though the inverse problem discussed assumes the field values are a low frequency, it is not assumed that the fields are static. However, it should be reasonable to use data from static field computations. Even though it does not exactly reflect the reality of the actual situation, it is a reasonable approximation. If we assume that $\omega=0$ the Maxwell's equations are

$$\nabla\times\vec{E}=0 \tag{3.21}$$

$$\nabla \times \vec{H} = \sigma \vec{E} + \vec{J} \tag{3.22}$$

The first of these two equations gives $E = \nabla\phi$ for some scalar function ϕ as discussed in chapter 1. If the divergence of the second of these equations is taken on both sides, we have

$$-\nabla \cdot \sigma \nabla \phi = \nabla \cdot J \tag{3.23}$$

This equation can be solved using an integral equation approach. With this type of solution method, computing the direct data with a piecewise constant conductivity σ is not difficult. The solution can be found using a boundary integral method [21][12]. The electric potential is found from the equation

$$\frac{\sigma_k^{'} + \sigma_k^{''}}{2} V(x) = \sigma_n V_0(x) - \sum_{j=1}^{n} \frac{\sigma_k^{'} - \sigma_k^{''}}{4\pi} \int_{S_j} V(x') n(x') \cdot \frac{x - x'}{|x - x'|^3} dS_j \tag{3.24}$$

where $\sigma_k^{'}$ and $\sigma_k^{''}$ are the conductivities on the inner and outer sides of the surface S_k respectively. Also, V_0 is the electric potential of a quasi-static dipole in an infinite homogeneous space which is given by the following

$$V_0(x) = \frac{1}{4\pi\sigma} p \cdot \frac{x - x'}{|x - x'|^3} \tag{3.25}$$

Of course to find the electric field we just find ∇V. Next the integral equation for the magnetic field is

$$H(x) = H_0(x) - \frac{1}{4\pi} \sum_{j=1}^{n} (\sigma_k^{'} - \sigma_k^{''}) \int_{S_j} V(x') n(x') \times \frac{x - x'}{|x - x'|^3} dS_j \tag{3.26}$$

Here, the H_0 is the magnetic field of a quasi-static dipole in an infinite homogeneous space. The equation for H_0 is the following

$$H_0(x) = \frac{1}{4\pi} p \times \frac{x - x'}{|x - x'|^3} \tag{3.27}$$

The integral equation in this section can be used to model a situation where the conductivity is piecewise constant in a finite number of regions. In the thesis, only a oneinterface problem will be demonstrated. The reason being that performing a more complicated multi-interface problem would require too much computational resources.

3.6 Multiple Dipoles

It is also of interest in the field of biomedical imaging to identify the position and orientation of more than one dipole. The reason for this is that the epilepsy may also be caused by multiple small current discharges in the brain. Thus, if it is assumed that the epilepsy is always caused by one dipole current, this could lead to innaccuracies. The inverse method presented here can also identifiy multiple dipoles. The key is to find enough functions which satisfy the equation

$$\nabla \times \nabla \times u = i\sigma\mu\nabla\phi \tag{3.28}$$

3.7 Numerical Examples

The numerical examples given are simple, yet illustrate the efficacy of the inverse method. The first experiment is a situation with no physical boundaries. Data is measured on an artificial boundary. We continue by adding some noise to the measured data to illustrate the inherent stability of the inverse problem method. The second experiment uses data from a Born approximation. The third experiment is a

single interface geometry, where the data is measured on the surface of a conducting sphere in a vacuum. Finally, the last experiment shows that more than one dipole can be reconstructed as well. It should be noted, that the simplicity of the examples problems is no indictment of the inverse problem method presented in the paper. In order to perform more realistic experiments, all one needs is data from a more sophisticated direct solver. If the values from the fields are accurate the inverse method will give an accurate reconstruction.

In the experiments shown here, the dipole position and orientation are given in each respective subsection. The data used in the reconstruction, is the tangential components of the electric and magnetic fields produced by the dipole current as measured on the surface of a sphere with radius .3 (all distances are given in meters) centered at the origin. Next, random noise was added to the computed data to test the stability of the inverse problem method. The following tables give the results of the numerical experiment.

3.7.1 Experiment with Green's Function Data

The data used in the first experiment is from fields which satisfy Maxwell's equations in a homogeneous medium of infinite extent. The material parameters are $\varepsilon = 8.854 \times 10^{-12}$ farads/meter, $\mu = 4\pi \times 10^{-7}$ henrys/meter and $\sigma = .33$ mhos/meter. First, true data from the Green's function computation was used in 3.6 and 3.7 .

Table 1: Inverse computation of x_0 and p_0 using true data.

ω=1000 Hz	x_0^1	x_0^2	x_0^3	p_0^1	p_0^2	p_0^3
actual	0.03	0.01	-0.05	0.1	0.2	0.3
estimated	0.030012	0.00995	-0.05002	0.100008	0.200018	0.300023
relative error	0.0004	0.005	0.0004	0.00008	0.00009	0.000076

3.7.2 Stability in the Presence of Noise

Here we use the same data as that in the previous subsection, but we add some random noise. First, 5 percent random noise is added to all of the field values. Next, 10 percent random noise is added to the data. We can see that the results are very stable in the presence of this noise.

Table 2: Inverse computation of x_0 and p_0 with 5% random noise.

ω=1000 Hz	x_0^1	x_0^2	x_0^3	p_0^1	p_0^2	p_0^3
actual	0.03	0.01	-0.05	0.1	0.2	0.3
estimated	0.029857	0.009602	-0.04992	0.099997	0.200044	0.299998
relative error	0.013767	0.0398	0.0016	0.00003	0.00022	0.000006

Table 3: Inverse computation of x_0 and p_0 with 10% random noise.

ω=1000 Hz	x_0^1	x_0^2	x_0^3	p_0^1	p_0^2	p_0^3
actual	0.03	0.01	-0.05	0.1	0.2	0.3
estimated	0.029691	0.009241	-.049813	0.099874	0.200072	0.299974
relative error	0.0103	0.0759	0.00374	0.00126	0.00036	0.000087

3.7.3 Experiment with Born approximation Data

Here, we add the effect of a sperical shell of 1cm thickness which has conductivity $\sigma = .03$. We treat this as a perturbation and proceed to compute a first order approximation as desrcibed in section 3.5.2. Of course the approximation provides less accurate data than the prior Green's function data, but we see that the results are still very acceptable.

Table : Dipole field with Born approximation						
ω=1000 Hz	x_0^1	x_0^2	x_0^3	p_0^1	p_0^2	p_0^3
actual	0.05	0.05	0.05	0.1	0.2	0.3
estimated	0.050884	0.050036	0.050742	0.100747	0.201439	0.301881
relative error	0.01768	0.00072	0.01484	0.00747	0.007195	0.00627

3.7.4 Experiment with Quasi-Static Data

Here we will actually have a boundary surface. We use the boundary integral technique reviewed in section 3.5.3 to model a conducting sphere. Outside the sphere the conductivity is zero. The computation is performed by dividing the sperical surface into trianglar elements and assuming the potential V is constant over each element. Once V is computed we use this data to compute the field values E and H. Using this model represents a more realistic situation, but unfortunately the approximations make for the least accurate data yet. However, the results show that the reconstruction is still acceptable.

Table : Quasi-static dipole in conducting volume.						
ω=0 Mhz	x_0^1	x_0^2	x_0^3	p_0^1	p_0^2	p_0^3
actual	0.05	0.05	0.05	0.1	0.2	0.3
estimated	0.051715	0.051552	0.0514608	0.101401	0.201824	0.302289
relative error	0.0343	0.03104	0.029216	0.01401	0.00912	0.010763

3.7.5 Experiment with Multiple Dipoles

Here we just use data produced by two distinct dipoles in an infinite region. With one dipole there are 6 parameters to compute which is why we use six harmonic functions. For two dipoles, there are 12 separate parameters which means that the challenge here

is to produce 12 harmonic functions to use in the inverse problem method. Again we can see that the results are good.

Table : First of two dipoles in conducting volume.						
ω=0 Mhz	x_0^1	x_0^2	x_0^3	p_0^1	p_0^2	p_0^3
actual	0.05	0..05	0..05	0.1	0.2	0.3
estimated	0.050012	0.050367	0.050012	0.100036	0.200572	0.300029
relative error	0.00024	0.00734	0.00024	0.00036	0.00286	0.00097

Table : Second of two dipoles in conducting volume.						
ω=0 Mhz	x_0^1	x_0^2	x_0^3	p_0^1	p_0^2	p_0^3
actual	0.05	-0.05	0.05	-0.1	0.2	-0.3
estimated	0.050218	-0.050124	0.05029	-0.099975	0.200571	-0.299988
relative error	0.00436	0.00248	0.0058	0.00025	0.002855	0.00004

3.8 Conclusion

The results in the previous tables show that the method works when considering the important effects of a boundary surface. Also, it shows that the method works with quasi-static field values. This may be viewed as a limiting case of the asymptotic method.

Future experiments will test the method when the dipole current is situated in a more realistic geometry, such as a heterogeneous material which models a human head. The difficulty lies in the generation of accurate data from the solution of the forward problem. The inverse method is only as accurate as the electromagnetic field values input as data. The inverse method itself produces error from the asymptotic approximation which is small. Beyond that, the only error from the inverse problem

method is the accuracy with which the numerical integrations are performed and with which the system of equations 3.6 and 3.7 is solved.

Finally, it should be stressed that the numerical reconstruction here is done without any least squares fitting or iteration. Also, the reconstruction is done without a priori knowledge of the frequency ω. Only the low frequency assumption is necessary.

BIBLIOGRAPHY

[1] H. Ammari and G. Bao, *Identification of cracks by boundary measurements at low frequencies*, Inverse Problems **16** (2000), 133-143.

[2] H. Ammari, G. Bao and J. L. Fleming, *An Inverse Source Problem for Maxwell's Equations in Magnetoencephalography*, Submitted

[3] H. Ammari and J. -C. Nédélec, *Time-harmonic electromagnetic fields in thin chiral curved layers*, SIAM J. Math. Anal. **29** (1998), 395-423.

[4] H. Ammari and J. -C. Nédélec, *Time-harmonic electromagnetic fields in chiral media,* In: E. Meister (Ed.), Modern Mathematical Methods in Diffraction Theory and its Applications in Engineering, Peter Lang, 1997, 174-202.

[5] H. Ammari and J. -C. Nédélec, *Propagation d'ondes électromagnétiques à basses fréquences,* J. Math. Pures Appl. **77** (1998), 839-849.

[6] H. Ammari, S. Moskow, and M. Vogelius, *Boundary integral formulae for the reconstruction of electric and electromagnetic inhomogeneities of small volume,* submitted.

[7] D. Colton and R. Kress, *Time-harmonic electromagnetic waves in an inhomogeneous medium*, Proc. Royal. Soc. Edinburgh A. **116** (1990), 279-293.

[8] D. Colton and R. Kress, *Inverse Acoustic and Electromagnetic Scattering Theory*, Springer-Verlag, New York, 1992.

[9] D. Colton and L. Päivärinta, *The uniqueness of a solution to an inverse scattering problem for electromagnetic waves*, Arch. Rational Mech. Anal. **119** (1992), 59-70.

[10] M. Eller, V. Isakov, G. Nakamura, and D. Tataru, *Uniqueness and stability in the Cauchy problem for Maxwell's equations and elasticity systems*, preprint.

[11] A. S. Fokas, I. M. Gel-fand and Y. Kurylev, *Inversion method for magnetoencephalography,* Inverse Problems **12** (1996), L.9-L.12.

[12] M. Hämäläinen, R. Hari, R. J. Ilmoniemi, J. Knuutila and O. V. Lounasmaa, *Magnetoencephalography-theory, instrumentation, and applications to noninvasive studies of the working human brain*, Rev. Mod. Phys. **65** (1993), 413-497.

[13] S. He, *Frequency Series Expansion of an Explicit Solution for a Dipole Inside a Conducting Sphere at Low Frequency*, IEEE Transactions on Biomedical Engineering **45** (1998) 1-10.

[14] S. He and V. G. Romanov, *Identification of dipole sources in a bounded domain for Maxwell's equations*, Wave Motion **28** (1998), 25-40.

[15] D.E. Heim, *On the Track Profile in Magnetoresistive Heads*, IEEE Trans. on Magnetics **30** (1994), 1453- 1464.

[16] V. Isakov, *Inverse Source Problems*, Math. Surveys and Monographs, Series Vol. 34, AMS, Providence, R. I., 1990.

[17] Jin Au Kong, *Electromagnetic Wave Theory*, John Wiley and Sons Inc., New York, 1990.

[18] Sergey A, Nazarov and Boris A. Plamenevsky, *Elliptic Problems in Domains with Piecewise Smooth Boundaries*, Walter de Gruyter & Co., Berlin, 1994.

[19] P. Ola, L. Päivärinta and E. Somersalo, *An inverse boundary value problem in electrodynamics*, Duke Math. J. **70** (1993), 617-653.

[20] B.D. Reddy, *Introductory Functional Analysis*, Springer-Verlag, New York, 1998

[21] J. Sarvas, *Basic mathematical and electromagnetic concepts of the biomagnetic inverse problem.*, Phys. Med. Biol. **32** (1987) 11-22.

[22] E. Somersalo, D. Isaacson, and M. Cheney, *A linearized inverse boundary value problem for Maxwell's equations*, J. Compt. Appl. Math. **42** (1992), 123-136.

[23] Z. Sun and G. Uhlmann, *An inverse boundary value problem for Maxwell's equations*, Arch. Rational Mech. Anal. **119** (1992), 71-93.

[24] Y. Suzuki and C. Ishikawa, *A New Method of Calculating the Medium Field and The Demagnetizing Filed for MR Heads*, IEEE Trans. on Magnetics **34** (1998), 1513-1515.

[25] J. Sylvester and G. Uhlmann, *A global uniqueness theorem for an inverse boundary value problem*, Ann. of Math. **125** (1987), 153-169.

[26] J. Sylvester and G. Uhlmann, *The Dirichelet to Neumann map and applications*, Inverse Problems in Partial Differential Equations, SIAM, Philadelphia, 1990, 101-139.

[27] Chen-To Tai, *Dyadic Green Functions in Electromagnetic Theory*, IEEE Press, New York, 1994.

[28] Georgi P. Tolstov *Fourier Series*, Dover Publications, INC., New York, 1962.

[29] W. von Wahl, *Estimating* ∇u *by* div$u$ *and* $\nabla \times u$, Math. Meth. Appl. Sci. **15** (1992), 123-143.

[30] Shan X. Wang and Alexander M. Taratorin, *Magnetic Information Storage Technology*, Academic Press, San Diego, 1999